## Dynamic failure in solids

Interrelating microscopic and continuum approaches helps explain the mechanisms by which materials fracture: the growth and coalescence of microvoids, microcracks and shear instabilities.

#### Donald R. Curran, Lynn Seaman and Donald A. Shockey

All material failure is dynamic, almost by definition. It advances by rate processes that have threshold conditions and characteristic growth kinetics.

A solid specimen on which a deformation is imposed at an arbitrary rate can accommodate this deformation by six basic modes:

1 elastic distortion,

2 homogeneous plastic flow,

3 phase changes,

4 nucleation and growth of ductile microvoids.

5 nucleation and growth of brittle microcracks and

6 nucleation and growth of shear insta-

Modes 2-6 are rate processes that can lead to material failure, such as those illustrated in figures 1-4. Figure 1 shows brittle microcracks in impact-loaded Armco iron, and the photo on the cover of this issue of PHYSICS TODAY shows similar cracks in a transparent polycarbonate material, Lexan. In figure 2, a region of impact-loaded steel has undergone a reversible volume contraction due to the phase transition from body-centered cubic to hexagonal close-packed and back, and has also experienced modes 2, 4 and 6. Figures 3 and 4 illustrate ductile microvoid nucleation and growth in dynamically and quasistatically loaded aluminum and copper samples, respectively.

The rate process of dislocation dyin crystalline solids. The rate process of new-phase formation controls the kinetics of phase changes, and the rate processes

namics governs homogeneous plastic flow

associated with microscopic and submicroscopic flaws govern failure by fracture or the formation of shear instabilities. In very brittle materials such as glass, these flaws may be a few angstroms in size; in polymers, they may be individual molecular chains. However, most structural solids contain larger microscopic flaws, such as inclusions, grain boundaries, cracks and voids. In metals, inclusions are often segregated into clusters by fabrication processes such as rolling or extruding. In short, every solid has an inherent distribution of flaws of various sizes and orientations.

Microscopic flaws that are exposed to a combination of tensile and shear stresses will tend to become "activated" as opening cracks or voids that grow as long as the tensile stress remains above a threshold value. Microscopic flaws exposed to combined compressive and shear stresses, on the other hand, will tend to become activated as shear instabilities, because the compressive stresses inhibit the opening of the flaws.

Whenever large numbers of microscopic flaws are activated, the microscopic failure processes may be statistically averaged to provide a workable continuum description of failure. Such a statistical approach is productive in that it allows a quantitative description of damage without requiring a description of each individual flaw or crack.

In this article we will concentrate on deformation modes 4-6. We will briefly review and discuss the history of theories of fracture, both continuum and microscopic, and then describe some recent advances in the development and application of the microscopic rate theories. Computational simulations of experiments showing combined failure by homogeneous plastic flow, fracture and shear instabilities will be illustrated by examples. We will discuss the dependence of the failure-rate processes on microstructural variables, temperature and the strain rate. Finally, we will pursue briefly the implications of modern microscopic rate theories of fracture for future applications in fracture mechan-

#### Crack activation and growth

Much of what has come to be called fracture mechanics is concerned with the stability of macroscopic flaws or cracks in applied quasistatic stress fields. A flaw or crack is considered macroscopic if it is large compared with the grains and other microscopic structural features. The stability criteria used are descended from A. A. Griffith's original energy-balance approach.

Griffith postulated that a flaw is unstable if an incremental virtual growth of the flaw reduces the elastic energy stored in the specimen more than the incremental energy required to create the new virtual flaw surface. This approach has proven very fruitful for brittle materials, because for such materials the energy required to create new flaw surface (that is, to tear adjacent material apart) is a true material property and independent of specimen geometry. In the 1950's George Irwin and his co-workers (see, for example, the 1968 compendium<sup>2</sup> edited by Harold Liebowitz) showed that this fracture energy is equivalent to a more usable design parameter, the critical stress intensity at the crack tip. This can be determined for brittle materials by measuring the critical loads at which initial macroscopic cracks or notches of known size become unstable and begin to propagate.

Much of the work in fracture mechanics has been devoted to establishing the geometrical conditions under which valid

Donald R. Curran is the manager, Donald A. Shockey the assistant manager and Lynn Seaman a research engineer in the Shock Physics and Geophysics Group of the Poulter Laboratory, Stanford Research Institute, Menlo Park, Calif.

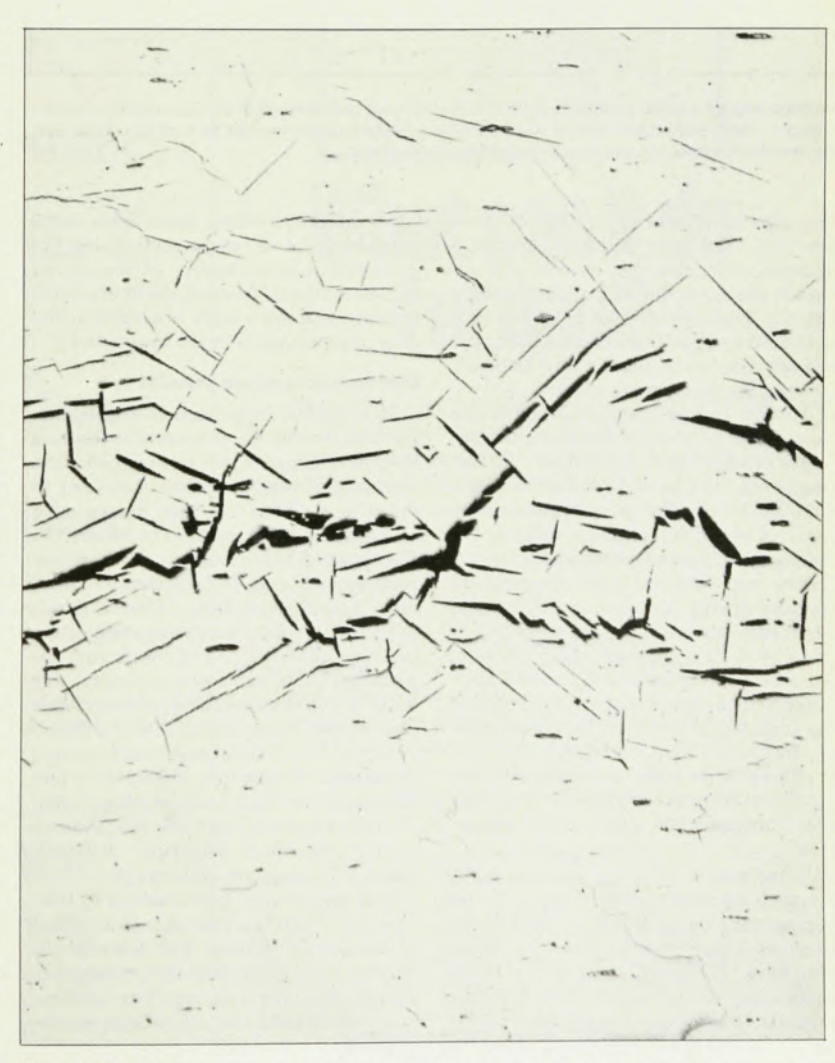
measurements of this critical value of the stress intensity factor at the crack front, called the "plane strain fracture toughness," can be made. The basic result is that the specimen dimensions must be large compared with the irreversible process zone at the macroscopic flaw boundary. This zone is defined here to be that region within which the stress concentration causes the occurrence of irreversible microscopic processes, such as plastic flow and microcrack activity.

The above result recently has been extended and generalized by James Rice<sup>3</sup> and others to cases in which the irreversible process zone is not small compared with the specimen dimensions. In such cases it has been shown that the so-called "plane stress fracture toughness,"  $K_c$ , can be replaced by a critical value  $J_c$  of a path-independent integral J.

In all these cases the processes occurring in the irreversible process zone are not treated explicitly. Rather, it is postulated that the energy required to extend the macroscopic flaw is a material property. That is, in suitably designed experiments the processes that lead to final separation of the material require an amount of energy per unit area of new surface that is independent of specimen geometry.

The microscopic rate processes may cause the macroscopic failure to be dependent on strain rate, and it is indeed commonly observed that  $K_c$  or  $J_c$  decrease as the rate of load application increases.

Concepts of fracture mechanics have also been applied to the *growth* of macroscopic flaws once they have become unstable. Again in the limit of small zones and large specimen dimensions, elastic continuum theory predicts that brittle tension cracks should quickly accelerate to a limiting velocity equal to the



Internal cleavage cracks caused by shock loading are revealed in this polished cross section of an Armco iron specimen. In the study of the way atomic-scale flaws grow into gross fractures, both microscopic and continuum approaches are useful.

Figure 1

Meniscus-shaped phase-transition region

Adiabatic shear bands

Incipient fracture damage

**Ballistic impact** against the top surface of this steel plug has resulted in several modes of deformation. The polished and etched cross section exhibits a phase change as well as plastic flow and the development of microvoids and shear instabilities. Figure 2

Rayleigh wave velocity (reference 2, volume II). However, in most structural materials the observed macrocrack velocities are much slower than this limiting velocity, partially because of plastic flow in the irreversible process zone. That is, the rate process of plastic flow partially governs the macrocrack velocity.

Another process often observed in this zone ahead of large propagating macroscopic cracks is that resulting in "surface roughness," the formation of microscopic voids or cracks the growth and coalescence of which define the advance of the macrocrack. On the continuum level, this results in an observed dependence of the fracture energy on crack velocity in experiments in which the load is applied so as to produce a constant crack velocity. An observed increase in fracture energy at high crack speeds is often attributed to the increase in crack-surface roughness. In short, the microprocesses in the irreversible process zone have changed character, resulting in a change in the energy that is required to advance the macrocrack.

When a static crack is impinged on by a travelling stress wave or pulse, its response may be quite different from its behavior when the same stress is applied statically. If the pulse duration is of the same order as, or smaller than, the time required for a sound wave to run the length of the crack, transient wave refraction effects are important. Several authors (see, for example, reference 4) have obtained analytic solutions for the

time-dependent elastic stress fields in the neighborhood of cracks undergoing engulfment by stress waves. However, the initiation criteria for such cracks are as yet unclear, and more work is needed in the area of stress-wave-crack interaction.

#### Microscopic fracture theories

In a parallel approach to continuum fracture mechanics, microscopic fracture theories attempt to describe explicitly the microscopic rate processes that lead to failure. Perhaps the best known such attempts are those reported by Serafim N. Zhurkov and his co-workers. Others (see references 6 and 7, for example) have taken a similar approach. Thus, a branch of physics is again faced with competition between microscopic and continuum approaches to the same phenomenon. We hope to avoid a repetition of this classic controversy by recalling that the development of the field of statistical thermodynamics, for example, linked the micro and macro worlds by constructing statistical distribution functions that average the rate at which molecular collisions transfer momentum and energy.

The microscopic rate theories of fracture do indeed use this approach. Rate equations are written that describe the average rate at which atomic bonds, molecular chains or incipient flaws are broken or activated, and algorithms are developed to relate this damage to continuum quantities such as stress, strain, and the engineering moduli and strengths.

To understand the link between con-

tinuum and microscopic theories we must first understand the governing microscopic processes. At the tip of a large crack, the kinetics of plastic flow, microcrack nucleation and growth determine the response of the irreversible process zone to the load. If the load is applied much more slowly than the relaxation times of these processes, the failure energy will be partitioned differently than if the load is applied at a rate comparable with the rate of the microprocesses. Although such effects can be handled by making the critical values of K or J functions of the strain or stress rates, this is not completely satisfactory, because rather simple rate processes can result in quite complicated dependencies of macrocrack energy on load history.

In short, both continuum and microscopic approaches have strengths and weaknesses. The main weakness of the usual continuum approach is that it requires the energy for advancing a macrocrack to be a material property, whereas the energy partitioning between competitive microscopic rate processes may in fact strongly depend on variables that are not material-specific.

A significant weakness of the microscopic-rate-process approach is that the actual parameters that govern the microscopic rate processes are difficult to observe and measure experimentally. Clearly, an important goal for fracture mechanics is to discover how to make such measurements. In this way a link between microscopic and continuum fracture mechanics could be forged, to the advantage of both. Let us look at recent progress along these lines.

#### Microcrack distributions

Our approach to microscopic fracture processes is an almost exact analogue of an approach used in dislocation dynamics. The field of dislocation dynamics, which describes the microscopic rate processes responsible for plastic flow of crystalline solids, was significantly advanced by W. C. Johnston and John Gilman<sup>8</sup> when they exposed lithium fluoride samples to pulse loads of known amplitude and duration, and observed how far individual dislocations moved. By this means they determined the average dislocation velocity as a function of applied stress and obtained the growth law for the rate process. They determined the nucleation (or multiplication) rate by counting the number of dislocations and determining the dependency of the dislocation concentration on applied stress and strain. They then combined the nucleation and growth rates for this microscopic process to form the link between the micro and the macro worlds, successfully describing continuum observations such as upper and lower yield points and work hardening.9 How can this method be applied to dynamicfailure data?

A common experimental way to observe

#### A World of Information at Your Fingertips



#### PHYSICS ABSTRACTS



Since 1898, the world's leading English-language Physics abstracting service. Published twice monthly, PHYSICS AB-STRACTS contains complete bibliographic information and full abstract on 100,000 items yearly, contained in over 3,000 alphabetical subject headings under 1,000 subject codes. Items are extracted from over

2,000 periodicals worldwide. Eight Indexes plus semiannual Author and Subject Indexes facilitate information access. Available in printed and microfiche editions. Back-volumes available on microfilm.

#### CURRENT PAPERS IN PHYSICS

Handy, inexpensive research tool—published twice monthly—contains full bibliographic information on over 60,000 items contained each year in PHYSICS ABSTRACTS. Issues do not contain the abstracts themselves. Comprehensive information access at a low cost. Reducedrate, personal subscriptions are available to all members of the AIP societies.



#### **INSPEC MAGNETIC TAPE SERVICES**

INSPEC's PHYSICS ABSTRACTS, ELECTRICAL & ELECTRONICS ABSTRACTS, and COMPUTER & CONTROL ABSTRACTS are also available on magnetic tape for computer information systems.

To receive INSPEC's 1977 brochure describing all of the INSPEC services, simply circle the Reader Service Card number listed below.

#### FOR FURTHER INFORMATION OR TO ORDER:

U.S., Canada and Latin America

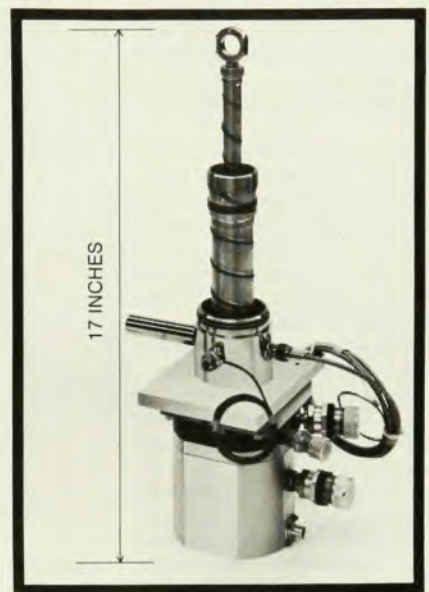
Ms. Catherine Ferrere INSPEC Marketing Department 445 Hoes Lane Piscataway, New Jersey 08854 (201) 981-0060 Ext. 121 or 122 Remainder of the World

Mr. Oliver Ball INSPEC Marketing Department Savoy Place London WC2R OBL, England (01) 240-1871 Ext. 305

Booth # 474, Physics Show

Circle No. 31 on Reader Service Card

# 10°K at the push of a button.



## What can it do for you?

A cryogenic cooling system that uses consumables is like an old-fashioned icebox. The DISPLEX® system is a refrigerator: a closed-cycle unit requiring only electricity (not gas or liquid cryogen).

Hundreds of chemists and physicists are using the DISPLEX because it is the best cryogenic cooling system you can buy in terms of performance, operating economy, convenience and versatility.

Just push a button to turn it on: it cools to 10°K in minutes. (Temperature variability with 0.1°K stability.) There are no dewar problems. The system is available to work when you need it.

Operating costs could hardly be lower: all you need is an electrical outlet. There are no consumables. The system is virtually maintenance-free. And it operates continuously without attention. Automatic temperature control and readout are built into the system.

Standard interchangeable interfaces (not shown) are available for IR, UV, Raman, Mossbauer, Cryopumping, ESR, X-ray and Faraday. But don't limit your thinking to these applications. Call for more information: at (215) 395-8355. Or write to Advanced Products Department, Air Products and Chemicals, Inc., P.O. Box 538, Allentown, Pa. 18105.



CRYOGENIC SYSTEMS

Circle No. 32 on Reader Service Card

microcracks or voids in incipient stages of nucleation and growth is to hit a flat specimen with a thin, flat flyer plate; this technique ensures uniaxial strain. Under such impact conditions each material element in the target specimen experiences a compressive pulse followed by a tensile pulse. In most homogeneous nonporous materials, the compressive pulse will not damage the material; however, the tensile pulse can nucleate and grow microcracks or voids, as shown in figures 1, 2 and 3, on pages 47–50.

The peak tensile stress experienced by the material will have about the same value for each material element of the target, but the duration of the tensile pulse will differ from point to point.7 This effect can be accentuated by tapering the flyer-plate thickness. The thick end and the thin end of such a tapered flyer will produce tensile pulses of different durations in the target material. Figure 5 shows sections of an Armco iron target hit by an Armco iron tapered flyer at an impact velocity of 0.1 km/sec; the impact compressive stress is 20 kbar. This figure illustrates that the material experiencing tensile pulses of longer duration produces larger, more numerous microcracks. Furthermore, the microcracks are numerous enough to make the use of statistical averaging feasible.

Microcrack and microvoid damage, such as is shown in figures 1 to 5 has been characterized and recorded in a variety of ways. Sometimes such damage is simply classified as "incipient," "intermediate" or "full spall," where, for example, the incipient level might be defined as one at which "microcracks are visible on a polished section at a magnification of 100." However, to obtain data in sufficient detail for input to, and correlation with, microscopic-rate-theory predictions, it is necessary to count and measure each microcrack and void.

Figure 6 shows an example of this method for an Armco iron target. The target was sectioned, as shown in the inset in this figure, and the length, orientation and distance from the impact plane of each crack were measured. For convenience in organizing the data, zones were marked off on the cross section. In the uppermost zone of the target, near the impact plane, there is little damage. The amount of damage increases as we proceed down through the zones until a plane of maximum damage is reached; the damage then decreases as we continue to the rear surface of the target. The peak tensile stress was approximately the same throughout the region of damage, but the duration of that stress varied in approximately the same way as the damage, having a maximum at the plane of maximum damage.

The observed cracks in each zone were organized into groups according to size and orientation angle. These surface distributions were then transformed sta-





A partial spall (dynamic rupture) is formed by the coalescence of voids in an aluminum plate of commercial purity. The photo on the left represents a width of about 5.0 mm; the tip of the crack is shown on the right at ten times higher magnification. Failure by void coalescence due to necking of the region between the voids in apparent near points marked "A."

Figure 3

tistically to volumetric distributions in size and angle. A sample set of volumetric crack distributions is shown in figure 6 for the zones shown in the inset. The angular variation is suppressed here, so that the ordinate is the total number of cracks larger than the indicated radius.

These distributions of crack sizes are approximated by the equation

$$N_g(R) = N_o \exp(-R/R_1) \tag{1}$$

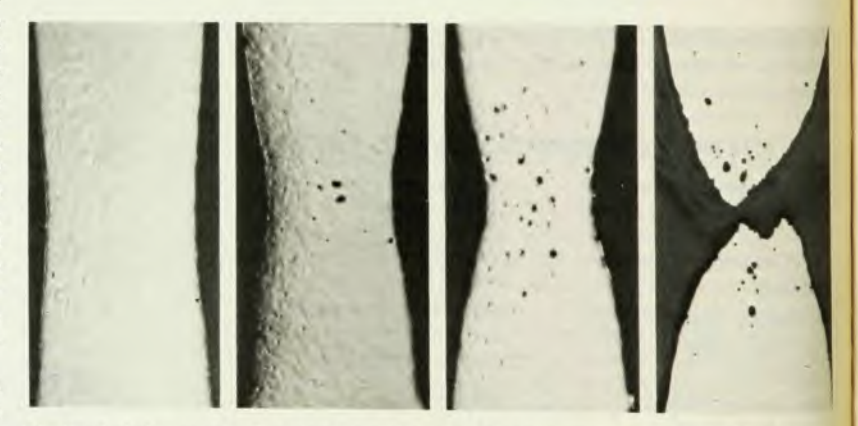
where  $N_{\rm g}$  is the cumulative number per cm<sup>3</sup> of cracks with radii larger than R,  $N_{\rm o}$  is the total number per cm<sup>3</sup> and  $R_{\rm 1}$  is a distribution-shape parameter.

Analysis of the results of plate-impact

experiments thus can provide detailed size and orientation distribution functions for the microcracks and voids. These distribution functions characterize the microscopic damage in a form suitable for inclusion in continuum theories. We will show below how this information can be used to construct rate equations for fracture, much as Johnston and Gilman<sup>8,9</sup> constructed rate equations for dislocation dynamics.

#### Rate theories

From a continuum viewpoint, the various microscopic rate theories of failure simply give an explicit time dependence



Plastic strain in copper. The polished sections show four stages in the rupture of three-quarters-hard tensile specimens of oxygen-free high-conductivity copper.

to the constitutive relations. These theories are of two basic types, passive and active. In the passive type, the degree of material failure depends on the stress or deformation history, but does not interact with or modify that history. The cumulative damage model of Floyd Tuler and Barry Butcher10 and the time-tofailure model of Zhurkov<sup>5</sup> are of this type. In the active type, the developing microscopic damage continuously degrades the material properties and causes stress relaxation to occur. The NAG (nucleation-and-growth) model developed by Troy Barbee and his collaborators at the Stanford Research Institute and the model of Lee Davison and Aldred Stevens,11 are of the active type.

Let us examine some of these theories and models in more detail:

Tuler-Butcher cumulative-damage model In its most general form, this popular model<sup>10</sup> states that the level of damage, D, depends on the stress history:

$$D = \int_0^t f[\sigma(t)]dt \tag{2}$$

Here  $\sigma$  is the stress and t the time; the form usually used for  $f[\sigma(t)]$  is

$$f[\sigma(t)] = A[\sigma(t) - \sigma_0]^{\lambda}$$
 (3)

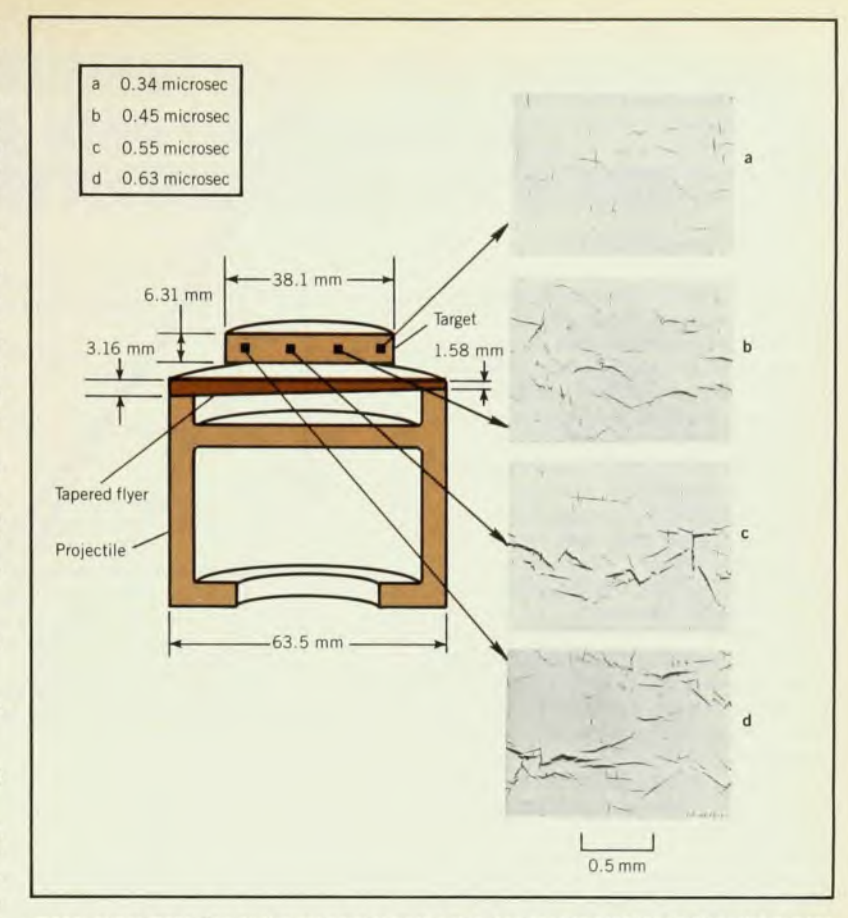
where A,  $\sigma_0$  and  $\lambda$  are material constants, and D is specified to be either a fairly qualitative level of damage, such as "observable cracks at  $100\times$ ," or a quantitative level such as a specified amount of degradation of modulus or strength.

The Tuler–Butcher model has been shown to be useful for a variety of metals where the loading conditions are not too far removed from those used to measure  $A, \lambda, \sigma_0$  and D, and when stress-relaxation effects are not important. However, where the stress pulse is strongly shaped by the developing damage, the passive nature of the model restricts its usefulness.

Zhurkov rate theory Zhurkov<sup>5</sup> and his co-workers have investigated the time to failure of strips and fiber bundles of a variety of materials exposed to tensile stresses over ten orders of magnitude in time: The shortest stress duration is of the order of 10<sup>-3</sup> sec, the longest about four months. Zhurkov found that his results for over fifty materials, including polymers and crystalline and polycrystalline metals, can be described by the formula

$$\tau = \tau_0 \exp[(U_0 - \gamma \sigma)/kT] \tag{4}$$

where  $\tau$  is the time to failure,  $\sigma$  the applied tensile stress, T the temperature and k Boltzmann's constant;  $\tau_0$ ,  $U_0$ , and  $\gamma$  are material constants. Zhurkov further found that  $\tau_0$  is about  $10^{-13}$  sec for all the materials; that is, of the order of the atomic vibration period. In addition,  $U_0$  was found to be equal to the binding energy of the atoms and  $\gamma$  to depend on the



Impact experiment. The configuration of the projectile, designed to produce uniaxial strain in the target, is shown in the diagram. The stress at any point is first compressive, then tensile. Use of a tapered flyer results in longer tensile pulses at the thicker end. As the cross sections **a**—**d** show, these longer pulses lead to greater damage in the Armco iron target. The inset gives the approximate durations of the tensile pulses.

amount of lattice disorder. Zhurkov thus presented his results as a theory involving the rate at which atomic or molecular bonds are broken. That is, we may rewrite equation 4 as

Number of bonds broken per sec per cm<sup>3</sup>

$$= \frac{n}{\tau} = \frac{n}{\tau_0} \exp\left[ (\gamma \sigma - U_0)/kT \right] \quad (5)$$

where n is the number of bonds per cm<sup>3</sup>. The exponential term in 5 is the probability that a bond will break, whereas  $n/\tau_0$  is the number of times per sec per cm<sup>3</sup> that an attempt is made to break a bond.

From equation 4 or 5 it can be seen that  $U_0/\gamma$  is a critical stress, because when  $\sigma \ge U_0/\gamma$ , the time to failure becomes equal to or less than one atomic vibration time. Therefore all bonds in the sample are broken in every atomic period, and the sample fractures immediately. However, solids do not generally fracture simultaneously at all atomic bonds, but they fail over a period of tenths of microseconds by the activation and growth of incipient flaws.

This discrepancy can be explained by noting that Zhurkov's shortest experimental loading time was of the order of a millisecond, long when compared with stress-wave propagation times in his specimens. Thus, his rate theory is basically for creep-rupture processes and can not be extrapolated into the region of very short times.

Nucleation-and-growth model An attempt to model the complete processes of nucleation, growth and coalescence of microvoids and cracks to form fragments at high strain rates has been carried out for a variety of solids by the present authors and our coworkers.7,12 In this approach data such as those of figure 5 are used to determine the rate equations for activation and subsequent growth of the incipient microscopic flaws in the material. As mentioned earlier, the cumulative size distribution of incipient flaws was found to be given by equation 1 for several metals, a polymer, quartzite rock and two composites.

The flaws are activated (microcracks or voids are nucleated) at a rate given by the formula

$$\dot{N} = \dot{N}_0 \exp \left[ (\sigma - \sigma_{\rm p0}) / \sigma_1 \right] \tag{6}$$

where  $\dot{N}_0$  is the threshold nucleation rate,  $\sigma_{n0}$  the tensile threshold stress and  $\sigma_1$  the stress sensitivity for nucleation. The average growth velocity of microcracks or voids was found for most of the materials studied to be given by

$$\dot{R} = \left(\frac{\sigma - \sigma_{\rm g0}}{4\eta}\right) R \tag{7}$$

where  $\sigma_{\rm g0}$  is the tensile-stress threshold for void growth (often equal to  $\sigma_{\rm n0}$ ) and  $\eta$ is the crack-tip viscosity that governs the growth rate for microcracks or voids. However,  $\dot{R}$  is not allowed to exceed the theoretical maximum growth rate equal to the Rayleigh wave velocity,  $C_{\rm R}$ .

In our work we observed that materials exhibiting microscopic damage in the form of microcracks (as opposed to microvoids) formed fragments as the microcracks coalesced. We constructed a model that described this coalescence and fragmentation process. The model, NAG-FRAG (Nucleation And Growth of cracks and resulting Fragmentation), has been used recently with promising results to predict cratering and fragmentation of rock by impacting projectiles and incontact explosive. 13

The NAG-FRAG model is of the active type; that is, it uses an algorithm in which the population of microcracks or microvoids increases the compliance of the material, thereby relaxing the stresses. The most important effect is the swelling of the material caused by the increased void fraction.

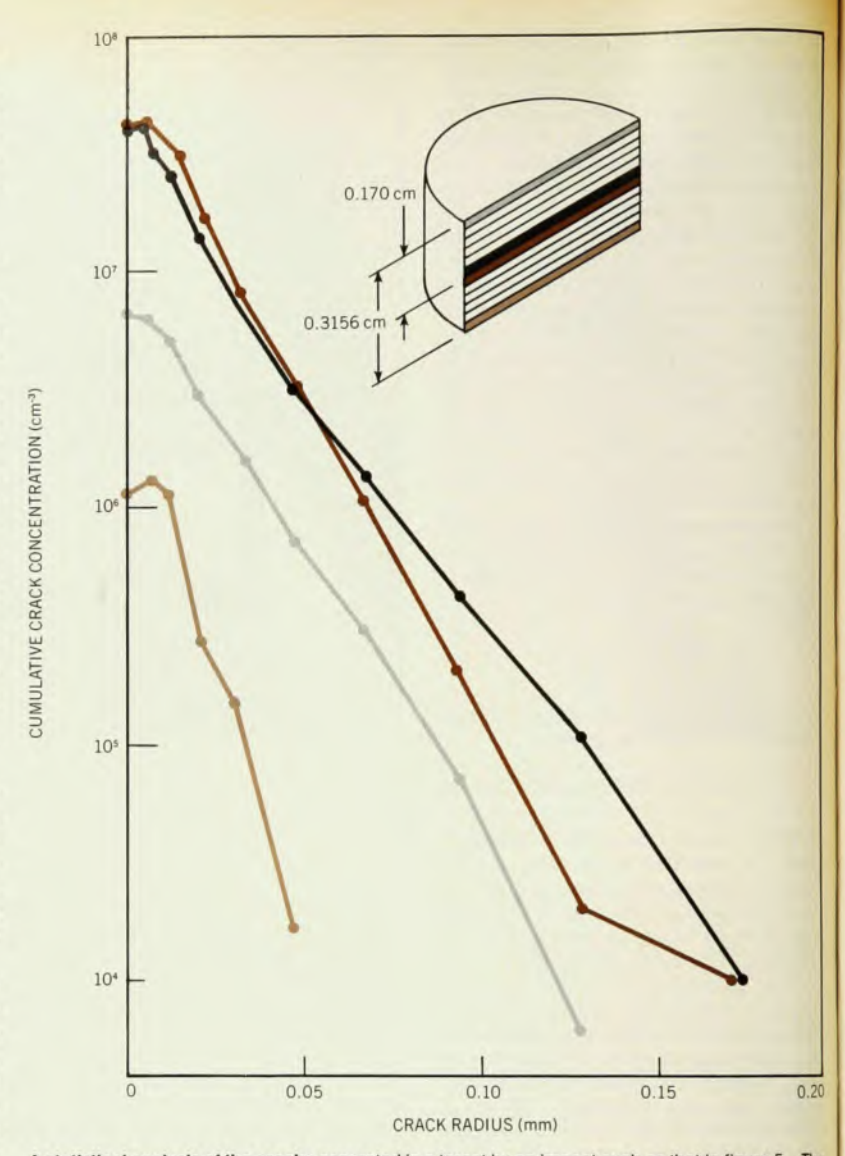
The importance of an active fracture model is illustrated by figure 7, which shows the computed stress path for an element of Armco iron subjected to a constant strain rate of  $1.3 \times 10^5 \,\mathrm{sec^{-1}}$ . If no stress relaxation were allowed, the stress-volume path would follow that determined by the laws of elasticity and plasticity, and the stress would increase indefinitely. However, the microcrack nucleation, growth and coalescence to fragmentation cause the stress to peak, decay and eventually reach zero. It is interesting to note the similarity between observed upper and lower yield phenomena and the description by dislocationdynamics theories.

Another interesting consequence of the approach given by equations 1, 6, and 7 is that the energy in a deforming cell of material can be computationally partitioned into the elastic, plastic and microfracture components,

$$\sigma_{ij} d\epsilon_{ij} = \sigma_{ij} \left[ d\epsilon_{ij}^{e} + d\epsilon_{ij}^{p} + d\epsilon_{ij}^{c} \right]$$
 (8)

where the total strain  $\epsilon_{ij}$  has been divided into these components. The microfracture strain,  $\epsilon_{ij}^{c}$ , is assumed to be purely volumetric and is obtained from the volumes of the opened microscopic voids and cracks.

A computation yielded a more detailed insight into this partition of energy in a



A statistical analysis of the cracks generated in a target by an impact such as that in figure 5. The target thickness is divided into 0.27-mm zones, as shown in the inset. The graph shows the size distributions in four of these zones, color-keyed to the diagram. The zones shown in black and in dark color, near the spall plane, exhibit the most severe damage; sections near the impact plane (gray) and the rear surface (light color) have fewer cracks.

fracturing cell of material. In this study, a cell was assumed to undergo uniform tension in all directions, so that plastic flow was suppressed. The energy was partitioned into elastic and fracture energies only. Computational simulations at several applied strain rates used the measured parameters for Armco iron in equations 1, 6 and 7.

The results show that the fracture energy depends strongly on the applied strain rate—for very high rates more energy is required to fracture the material. Furthermore, the applied energy first goes mainly into elastic energy, which is then converted to fracture energy.

If we now imagine a cell at the tip of an advancing microscopic notch or crack, a similar situation will clearly occur, this time complicated by plastic flow and its resulting energy. At high macrocrack velocities the energy used to advance the crack will be greater; in addition, it will partition differently than for slow macrocrack velocities.

#### **Analytic models**

As we discussed earlier, this is one reason why continuum fracture mechanics runs into difficulties for ductile materials. For them the strong dependence of the energy partitioning on the strain rate makes it difficult to consider the energy required to advance the macrocrack to be a material property, although it may in principle be handled by making the critical values of G and J complicated functions of the stress and strain histories.

### WHY AN INSTRUMENT MADE FOR MEASURING **ONE KIND OF RADIATION NEEDS A DETECTOR MADE FOR MANY.**

Because the detector made for many kinds of radiation happens to be the most accurate for each. And the most stable.

Galileo's line of Channeltron® detectors.

All of them possess the lowest dark current you can find (<0.5 counts/second).

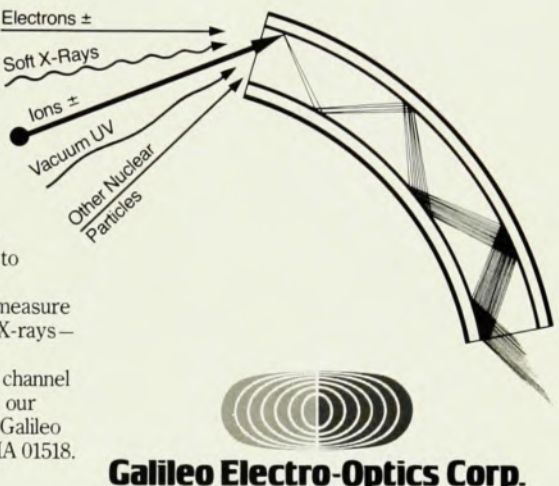
And they are the only detectors that are still dependable after repeated exposure to air.

There's more.

Our detectors come to you with a warranty and all the engineering assistance you need. Plus they can be made to almost any size or shape your application requires.

So now for all the very different instruments made to measure radiation - from nuclear particles to vacuum UV, to soft X-rays you need only one detector. From one source.

For more information about our standard line of single channel detectors, our Channeltron electron multiplier arrays, or our custom assemblies with associated electronics, write to Galileo Electro-Optics Corporation, Galileo Park, Sturbridge, MA 01518. Or better, call us (617) 347-9191.



Circle No. 34 on Reader Service Card

### **YOUR SOURCE FOR** IPTICS

- Optics and Windows in fused quartz, glass and sapphire
- Prototype and production capabili-
- Commercial and precision finishes Many catalog items in stock

including LENSES, MIRRORS, WIN-DOWS, BEAM SPLITTERS, PRISMS, FILTERS & OPTICAL FLATS. Spe-cialists in finishing glass and quartz



Free catalog on request

171 Oak Ridge Rd., Oak Ridge, N.J. 07438

Circle No. 35 on Reader Service Card

## A NEW PORTABLE



- 121/4 pounds
- · 61/2 × 81/2 × 121/2" cabinet
- · 25 watts total power
- 1024 × 10<sup>6</sup> memory divisible by 1/8's
- · Dual cursors
- · Multiple region of interest
- Integral CRT
- · Alphanumeric display
- 10MHZ 10 μsec MCS
- PHA. MCS. & Mössbauer

All of the classical MCA features and many new ones.

#### RELIABLE?

An industry first 18 month warranty!

#### LO COST?

You bet!

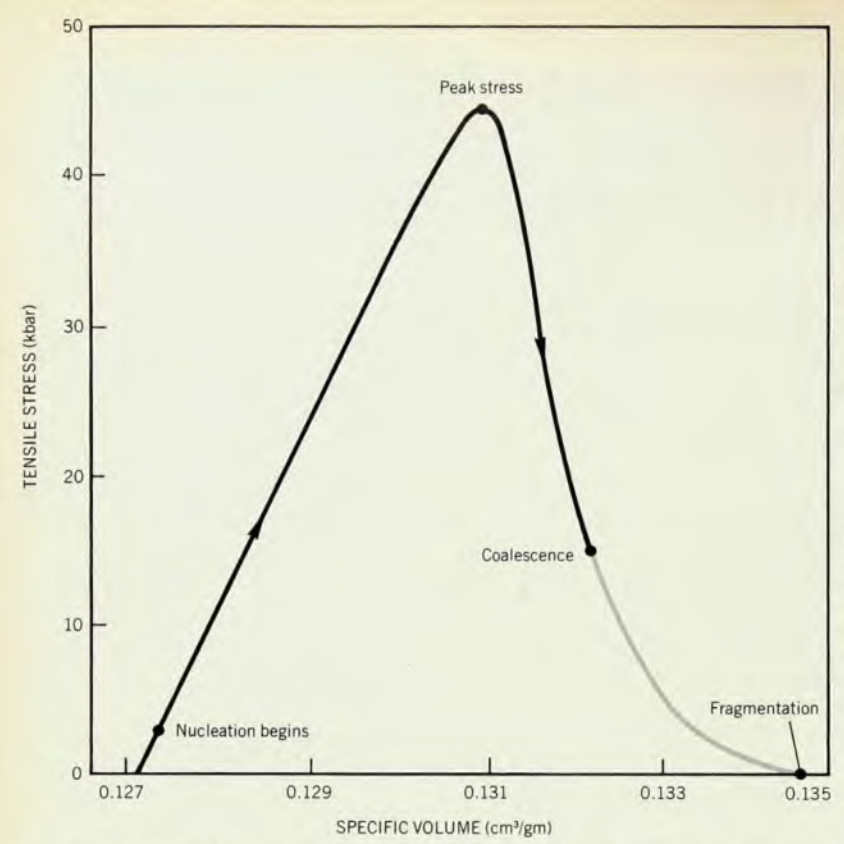
D. S. Davidson Co. 333 State Street North Haven, Conn. 06473

(203) 288-7324

Booth #425, Physics Show

Call or write:

Circle No. 36 on Reader Service Card



Stress-volume path of Armco iron loaded to fragmentation at constant strain rate. The gray line marks the region in which fragmentation progresses by microcrack coalescence. Figure 7

The NAG-FRAG model discussed above is applied directly in wave-propagation computer codes and is therefore not described in the classical continuum-mechanics format, of complete integral expressions relating stresses, strains, entropy, energy and continuum measures of microscopic damage.

There is in fact a reason to avoid such integral formulations. Wave-propagation codes step forward in discrete time steps, enforcing discrete changes in all the state variables, which in turn means that the constitutive relations may be used in differential form, so that the increment in stress is a function of the increments in the state variables. Such differential constitutive relations are much easier to use than those in which the total stress is expressed as a function of the complete history of the state variables. They can easily accommodate nonlinear and hysteretic effects such as plasticity and fracture, and history effects such as complicated loading paths pose no special problems.

On the other hand, the integral constitutive relations have the possible advantage of providing easier insight into the interactions of the effects of the different state variables. Such analytic constitutive relations also may be more easily tested for thermodynamic consistency. A start on construction of such thermome-

chanical constitutive relations, including a continuum description of developing microscopic damage, has been made by Davison and Stevens, 11 who describe the microscopic damage by a finite number of vector fields, considered to be internal state variables. Because the stress tensor, entropy, Helmholtz energy and heat flux depend on these fields as well as on the other state variables, this damage model is of the active type: Developing damage has a direct effect on the dependent variables and can provide the required stress relaxation.

Davison and Stevens<sup>11</sup> have shown that many of the observed features of microscopic fracture processes can be cast into this analytic form. However, the basic difficulty remains, of combining a damage description with other nonlinear effects such as plasticity and other hysteretic effects; in their applications they also use their constitutive relations in differential form with finite-difference wave-propagation codes.

In our opinion, constitutive relations of the differential type combined with wave-propagation calculations will continue to be very useful for applications where the nonlinear histories of the state variables are important.

As we mentioned earlier, another important microscopic failure process at high strain rates is the nucleation and growth of shear instabilities such as shear cracks and "adiabatic shear bands." Adiabatic shear bands, which occur in solids undergoing plastic deformation at a high rate, were discussed as early as 1944 by Clarence Zener and J. H. Hollomon, 14 Shear instabilities form when localized plastic flow around inherent flaws or other stress raisers cause localized heat-When the loading rate is high enough there is insufficient time for the heat to flow away from the local "hot spot." If the heating is sufficient to soften the material, additional plastic flow will occur, and the process will feed on itself and become unstable.

#### Shear instabilities

Using the same philosophy as the one behind the NAG-FRAG approach, the present authors have constructed a preliminary model to describe the nucleation and growth of adiabatic shear bands. In this model, called SNAG (Shear Nucleation And Growth), the size distribution of the nucleated shear bands is again given by equation 1. The observed shear instabilities propagate through the plastically deforming material with geometries like macroscopic edge dislocations. This allows use of the Orowan equation:

$$\dot{\gamma}_{\rm p} = NBV$$
 (10)

where  $\dot{\gamma}_{\rm p}$  is the plastic strain rate, N the number of shear bands intersecting a unit section through the material, B the jog accommodated by the band and V the average band velocity. The shear-band velocity is assumed to be of the form

$$V = A \dot{\gamma}_{\rm p} R \tag{11}$$

where R is the band length (distance travelled) and A is a material property.

Another key assumption in the model is that once such bands are formed, all the plastic work goes into the bands. The bands are heated to the temperature that corresponds to complete loss of material strength by thermal softening. In the present form of the model, the condition for the initiation of such shear instabilities is that both a critical strain and a critical strain rate be exceeded. Furthermore, NAG and SNAG are mutually exclusive. If the threshold conditions for microscopic fracture are met first, only fracture occurs in a given material cell, and vice versa.

An algorithm similar to that for microcracks allows intersecting shear bands to cause fragmentation. The increase in material compliance with band density causes stress relaxation.

Although still under development, the SNAG model, when combined with NAG-FRAG, has given promising agreement between observed and predicted fragment-size distributions for explosive-filled iron and steel cylinders, as figure 8 illustrates. In these computations, the cylinders were correctly predicted to experience fracture in their

outer portions and shear banding in their inner portions. The dominant orientation of the microfractures, with the normals to the cracks mostly in the circumferential direction, was also correctly predicted. The NAG-FRAG-SNAG model therefore appears adequate to describe dynamic failure by combined microcracking and shear banding.

#### Microstructure and temperature

The microscopic-rate-process approach to material failure, based on the observation that failure is governed by activation and growth of inherent flaws in the material, provides a natural link between failure and microstructure. If we can identify the dominant flaws in a material, we can begin to understand the role microstructural features play in the fracture process and suggest ways to design materials to better resist failure.

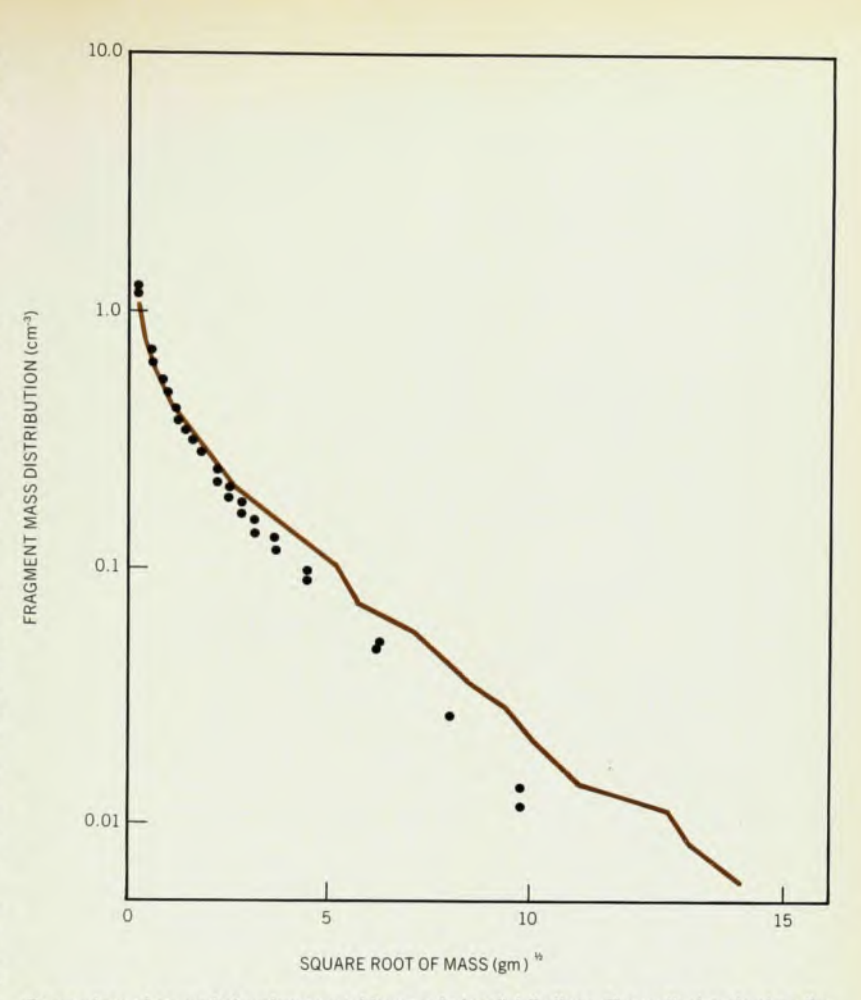
To attain this exciting goal, however, is not so simple because, while for some materials the flaw structure is easy to identify and measure, <sup>13</sup> for others the dominant flaws and their activation processes are difficult to quantify. In a 1973 review <sup>15</sup> we discussed microfracture nucleation at grain boundaries, precipitates inclusions, second-phase particles and voids. In addition to these microscopic nucleation can occur at dislocation pileups or impurities.

According to the NAG model, <sup>15</sup> the main features of microfracture activity are governed by the material properties  $R_0$ ,  $\sigma_{n0}$ ,  $\sigma_1$ ,  $N_0$ ,  $\sigma_{g0}$  and  $\eta$  in equations 1, 6, and 7. The quantities  $N_0$  and  $R_0$  are directly related to the inherent flaw size and number distribution, and  $\sigma_{n0}$  and  $\sigma_{g0}$  to strength and stress concentration around the flaws. The stress sensitivity nucleation  $\sigma_1$  is also related to the number and size distribution of the inherent flaws. The resistance to microcrack growth  $\eta$  is a complicated function of the obstacles to microcrack growth and is not well understood.

Most of these NAG material properties depend on temperature. For example, for S200 beryllium at 540 deg C,  $N_0$  was below its room-temperature value, whereas  $R_0$  and  $\eta$  had increased. The dependency of these microfracture parameters on microstructural features and temperature forms an exciting area for research, but is not well understood yet.

#### A powerful addition

In this survey we have reviewed current theories of material failure and presented recent advances in the modelling of the microscopic rate processes that govern failure on the continuum scale. The boundary between classical continuum fracture mechanics, based on the energy-balance approach, and the microscopic-rate-process approach has emerged as an especially interesting topic. For very brittle quasistatic fracture, where the



Comparison of computed and measured fragment-size distributions. The vertical scale gives the number per cm³ of fragments with mass greater than the specified value. The data points are from two experiments on cylinders with inside and outside diameters of 7.62 cm and 11.43 cm, filled with the solid explosive "composition B." The colored line is computed.

irreversible process zone is small compared with macrocrack dimensions and specimen size, the classical energy-balance approach is clearly to be preferred. On the other hand, for many structural materials and applications, this zone is large and consists of many microscopic voids and cracks rather than a single macroscopic crack front. For these cases, and for dynamic cases where many flaws are simultaneously activated, the microscopic-rate-process approach promises to provide a powerful addition to fracture mechanics.

The computations presented were performed by Michael Austin and the micrographs displayed were made by Dante Petro.

#### References

- A. A. Griffith, Phil. Trans. 221, 163 (1921).
- Fracture, volumes I-VII (H. Liebowitz, ed.), Academic, New York (1968–1972).
- 3. J. R. Rice, J. Appl. Mech. 35, 379 (1968).
- L. B. Freund, J. Mech. Phys. Solids 21, 47 (1973).

- S. N. Zhurkov, Int. J. Fracture Mech. 11, 5 (1975).
- G. J. Dvorak, in *Dynamic Crack Propagation* (G. C. Sih, ed.), page 49, Noordhoff International, The Netherlands (1973).
- T. W. Barbee Jr, L. Seaman, R. Crewdson,
   D. R. Curran, J. Materials 7, 393 (1972).
- W. G. Johnston, J. J. Gilman, J. Appl. Phys. 30, 129 (1959).
- 9. W. G. Johnston, J. Appl. Phys. 33, 2716
- F. R. Tuler, B. M. Butcher, Int. J. Fracture Mech. 4, 431 (1968).
- L. Davison, A. L. Stevens, J. Appl. Phys. 44, 668 (1973).
- D. R. Curran, D. A. Shockey, L. Seaman, J. Appl. Phys. 44, 4025 (1973).
- D. A. Shockey, D. R. Curran, L. Seaman, J. T. Rosenberg, C. F. Petersen, Int. J. Rock Mech. Sci. and Geomech. Abstr. 11, 303 (1974).
- C. Zener, J. H. Hollomon, J. Appl. Phys. 15, 22 (1944).
- D. A. Shockey, L. Seaman, D. R. Curran, in Metallurgical Effects at High Strain Rates (R. W. Rohde, B. M. Butcher, J. R. Holland, C. H. Karnes, eds.), Plenum, New York (1973).